# We are IntechOpen, the world's leading publisher of Open Access books Built by scientists, for scientists

**4,800**
Open access books available

**122,000**
International authors and editors

**135M**
Downloads

Our authors are among the

**154**
Countries delivered to

**TOP 1%**
most cited scientists

**12.2%**
Contributors from top 500 universities

CLARIVATE ANALYTICS BOOK CITATION INDEX INDEXED

WEB OF SCIENCE™

Selection of our books indexed in the Book Citation Index in Web of Science™ Core Collection (BKCI)

## Interested in publishing with us?
## Contact book.department@intechopen.com

Numbers displayed above are based on latest data collected.
For more information visit www.intechopen.com

# 9

# A Tunable Microfluidic Device for Drug Delivery

Tayloria Adams*, Chungja Yang*, John Gress,
Nick Wimmer and Adrienne R. Minerick
*Michigan Technological University*
*USA*

## 1. Introduction

The field of microfluidics, small-scale tests from nanoscale to microscale, has grown dramatically over the past two decades as evidenced by greater than 30,000 papers published over the last 10 years on the topic [Web of Knowledge search using 'microfluidic' terms October 2011]. Microfluidic platforms, also known as lab-on-a-chip (LOC), include a set of miniaturized integrated unit operations that are touted to lead to fast, easy, precise control in biological and chemical systems. LOCs include the development of point-of-care (POC) medical diagnostic devices with the advantages of increased sensitivity, lower sample volumes, lower reagent volumes, low energy, low cost, low labor need, and less likelihood of human error (Xiao & Young, 2011). Due to these advantages, LOCs have substantial potential to be widely utilized in medicine for analytical and diagnostic assays, biosensors, and drug delivery.

Microfluidic technology has been used for a wide variety of applications such as forensics, cell phone facilitated micro-imaging, and analytical testing. In 2006 Bienvenue at al., compared the use of microfluidic technology with a commercial kit that utilized dithiothreitol to extract and purify DNA from sperm samples. The sample volume was less than 10 μL and the resulting electropherograms were very similar for both techniques (Bienvenue et al., 2006). DNA separation has also been studied by Aboud et al. Pentameric short tandem repeat (STR) markers were tested in a microfluidic device on single-stranded DNA. Coupling microfluidics with pentameric STRs improved allele resolution by 3.7 times (Aboud et al., 2010). In these cases, microfluidics can be used as a rapid screening tool for forensic DNA analysis to help resolve the backlog of DNA casework (Aboud et al., 2010; Bienvenue et al., 2006). Zhu et al., combined optofluidics with cell phone technology. A cell phone was converted to a microscope analysis tool by integrating optofluidic fluorescent cytometry with compact optical attachments. The cell phone optical attachment included a lens, plastic color filter, two light emitting diodes, and batteries, which altogether weighed less than 1 lb. To test the effectiveness of this new imaging system, the density of white blood cells were measured using the cell phone-based fluorescent image cytometry and compared with the white blood cell density found with a commercial hematology analyzer.

* These authors contributed equally

The blood sample was injected into the microfluidic chamber using a syringe pump and the cell phone recorded the fluorescent emission. This study demonstrated that the densities found by both systems were a good match with less than 5% error and that cell phone optofluidic fluorescent imaging cytometry was useful for rapid blood cell counts or screening of water quality (Zhu et al., 2011).

Research into microfluidic devices tailored for the medical field is extensive. Weng et al., developed a suction type microfluidic device to detect the dengue virus. This three-layer device used pneumatics, mixing, and transport to detect the virus in 30 minutes (Weng et al., 2011). Digital microfluidic devices transport biochemical materials in the form of miniature discrete droplets (Xiao & Young, 2011) and have been used for immunosensing, proteomics, DNA, and cell based assays (Vergauwe et al., 2011). Dielectrophoresis (DEP) has been incorporated into microfluidic devices for transport, separation, and blood typing (Minerick et al., 2008; Srivastava et al., 2011; C. Wang et al., 2011). DEP phenomena is the movement of cells from an external applied electric field and has been used to continuously separate breast cancer cells from normal blood cells (Alazzam et al., 2011). The device developed by Alazzam et al. can potentially be used as an early detection method for cancer.

Professor Robert Langer and other researchers at MIT investigated the idea of a "pharmacy on a chip". They performed controlled release studies to determine if a microfluidic platform could act as a pulsatile release drug delivery system. Pulsatile release is a common controlled release method used to treat people with disorders that require drugs to be delivered at varying rates over time. A prototype microchip made from silicon was developed. The microchip had multiple reservoirs for drug storage and the reservoirs were covered with gold membranes. The reservoirs were filled with sodium fluorescein and calcium chloride using ink jet printing. To release the drugs an electric potential of approximately 1V was applied and the gold membranes were dissolved in 10 to 20 seconds. The results from this study revealed that storage and on-demand delivery of drugs can be achieved from microfluidic LOC technology. One major advantage of using microfluidic platforms for drug delivery is that small microchips can be implanted inside the body to locally treat diseases (Santini et al., 1999, 2000). Farokhzad et al. gave a possible application of microfluidic technology in the field of urology (Farokhzad et al., 2006). Other researchers have implemented the proof-of-concept that Langer demonstrated for ambulatory emergency care treatment. A plethora of drug delivery systems that can be embedded in the body have been researched for use in chronic and non-chronic diseases. When treating chronic and non-chronic diseases drugs are delivered over long periods of time. These systems are now modified to rapidly deliver drugs in emergency situations (Elman et al., 2009). Elman et al. developed a smart microchip implant to deliver a drug bolus when disease symptoms are detected. The device is composed of three layers: reservoir layer where drug solution is stored, membrane layer where reservoir is sealed and location of drug is released, and actuation layer where bubbles are formed to trigger the release of the stored drugs. The actuation layer triggers the operation of the device. Micro-resistors heat the drug to generate bubbles, pressure is produced, and the membranes burst delivering the drug (≈ 20 μL) rapidly from the device to its target area in 45 seconds. In this work vasopressin was used as the drug and it was found that 92.5% of the solution loaded into the device was released. Devices of this nature have the potential to accompany cardiac devices such as defibrillators and pacemakers (Elman et al., 2009). Langer's findings have even been

extended to nanotechnology. Brammer et al., has shown that silicon nanowires are a viable drug delivery system for antibiotics. It was shown that silicon nanowires sustained drug release levels for 42 days (Brammer et al., 2009).

Despite this wide breadth of research success, commercial implementation of POC devices for diagnostics assays, biosensors, and drug delivery have been much slower than originally predicted. A feature article in Time magazine in 2001 exemplified this dream touting safer and more effective drug delivery techniques (Bjerklie & Jaroff, 2001). However, only a few notable LOC platforms have come to market and are most advanced in the areas of bioassays (pregnancy/ovulation tests, etc.) and gene chips. Bioassay companies include eBioscience (http://www.ebioscience.com/), and Chembio Diagnostic Systems, Inc. (http://www.chembio.com/). Notable gene profiling chips include those by Affymetrix **(**http://www.affymetrix.com/), Fluidigm (http://www.fluidigm.com/snp-genotyping. html), Gyros (http://www.gyros.com/en/home/index.html), and Sage (http://www. sagescience. com/). Blood chemical analyzers are marketed by PiccoloXpress (http:// www.piccoloxpress.com/), while versatile analytical LOCs are marketed by Caliper (http://www.caliperls.com/products/labchip-systems/) and Dolomite Microfluidics (http://www.dolomite-microfluidics.com/). Commercialization is more advanced in the diagnostics arena than in the drug delivery area due to the complexity of sensing the concentration of the drug and controlling the release of new drug. However, as demonstrated by the growth in foundational research, popular news source stories, and commercialization of products, new innovations in this area are being sought.

Cancer is a disease that touches everyone in the world; people are either directly affected by cancer or know someone suffering from the disease. Globally, cancer is responsible for 1/8$^{th}$ of all deaths, which is more than HIV/AIDS, malaria, and tuberculosis combined (American Cancer Society, 2011). It is estimated that 1.5 million new cases of cancer will be diagnosed in the U.S. in 2011. Cancer is growing at an increasingly high rate and it is expected that there will be 21.4 million new cases of cancer in 2030 and 13.2 million cancer deaths (American Cancer Society, 2011). Gastric cancer is malignant cell growth originating in the gastro-intestinal tissue lining and kills 650,000 people with 870,000 new cases diagnosed annually (Balcer-Kubiczek & Garofalo, 2009). It is the second most fatal disease in the world (Balcer-Kubiczek & Garofalo, 2009; National Cancer Institute, 2010) and has a poor prognosis due in part to late stage development of any symptoms. People diagnosed with gastric cancer often do not experience symptoms until the disease is metastatic and spreading elsewhere in the body. This then dictates systemic chemotherapy treatment, which traditionally is conducted with regular injections or an embedded catheter. These methods add suffering and additional pain beyond the discomforts of chemotherapy. Further, these methods of drug delivery have large variations in patient exposure concentrations over the course of the treatment; survival rates for gastric cancer suggest this approach is not entirely effective. Therefore, there is a great need for development of new technology to treat cancer patients. The new technology should have two goals **(1)** *effectively treat cancer patients to eradicate disease* and **(2)** *make cancer treatments as painless and noninvasive as possible*. Here we wish to combine four unique technologies into a microfluidic device to provide novel nanoscale drug delivery for cancer patients via a wrist device resembling a watch. Figure 1 shows the global view of our chemotherapy drug delivery system and Figure 2 shows how these four technologies fit together on the drug-delivery microfluidic device and are then discussed separately in the following sections.

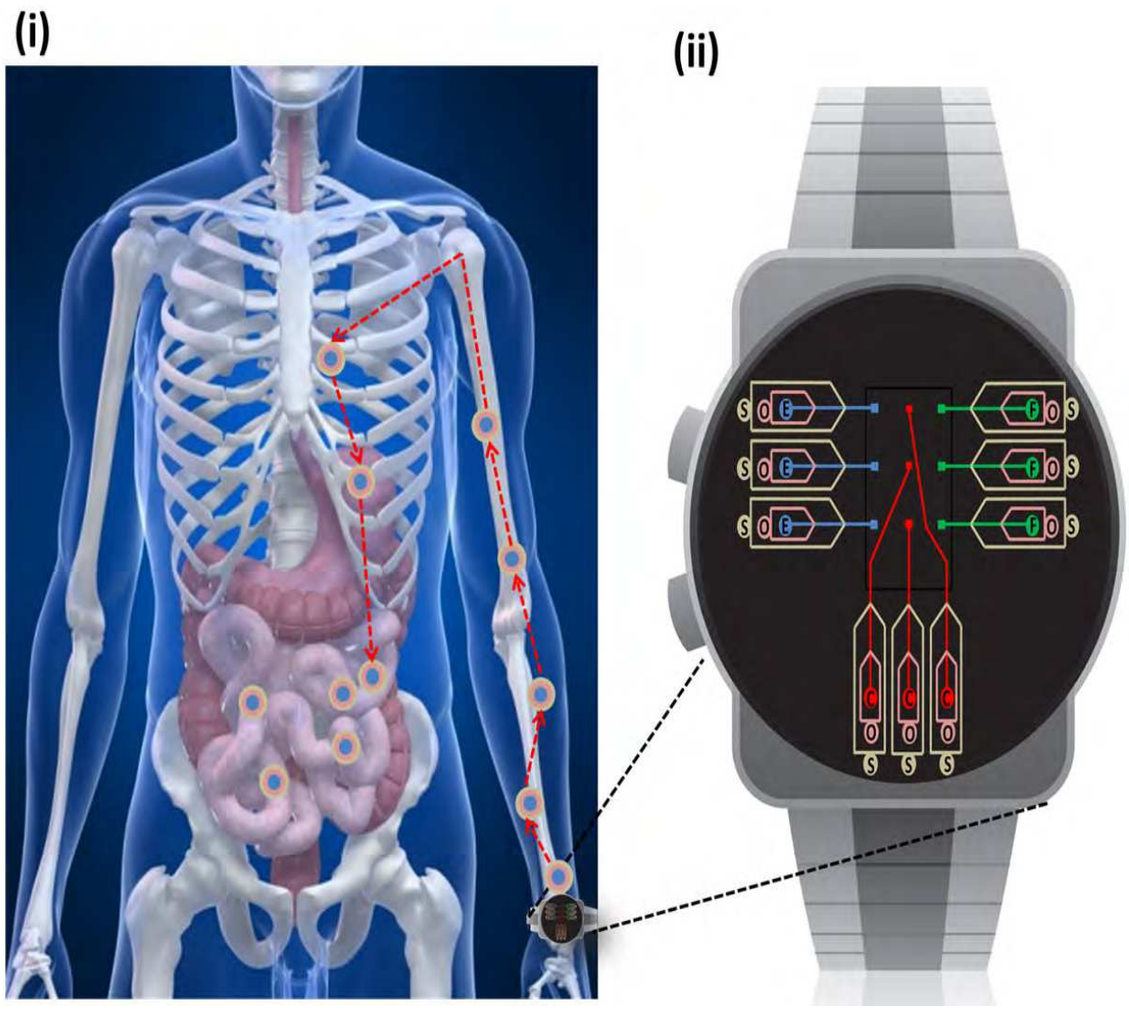


Fig. 1. Global view of chemotherapy drug delivery system, (i) path of emulsified drug from the wrist microdevice through the human body and (ii) enlarged view of wrist device depicting the chemotherapy drug delivery system. The encapsulated chemotherapy drug droplets travel from the wrist device to the intestines contacting circulating tumor cells (CTCs) to treat the gastric cancer.

In Figure 2(i), the reservoirs for each drug are centralized into larger chambers above the layers shown in Figure 2(iv). There is a primary and three secondary reservoirs for oil (one for each drug), and the same for saline. The primary reservoir allows the flow rate of each drug to be independently controlled. This device uses microchannels and tunable electrodispersion to form in-line emulsions of the chemotherapy drug, which are then delivered to the patient using adjustable dielectrophoretic pumping and painless microneedles that penetrate the dermis of the skin. The focus of this new technology has been to specifically treat gastric cancer, but can be adapted to treat many other types of cancer and possibly other diseases.

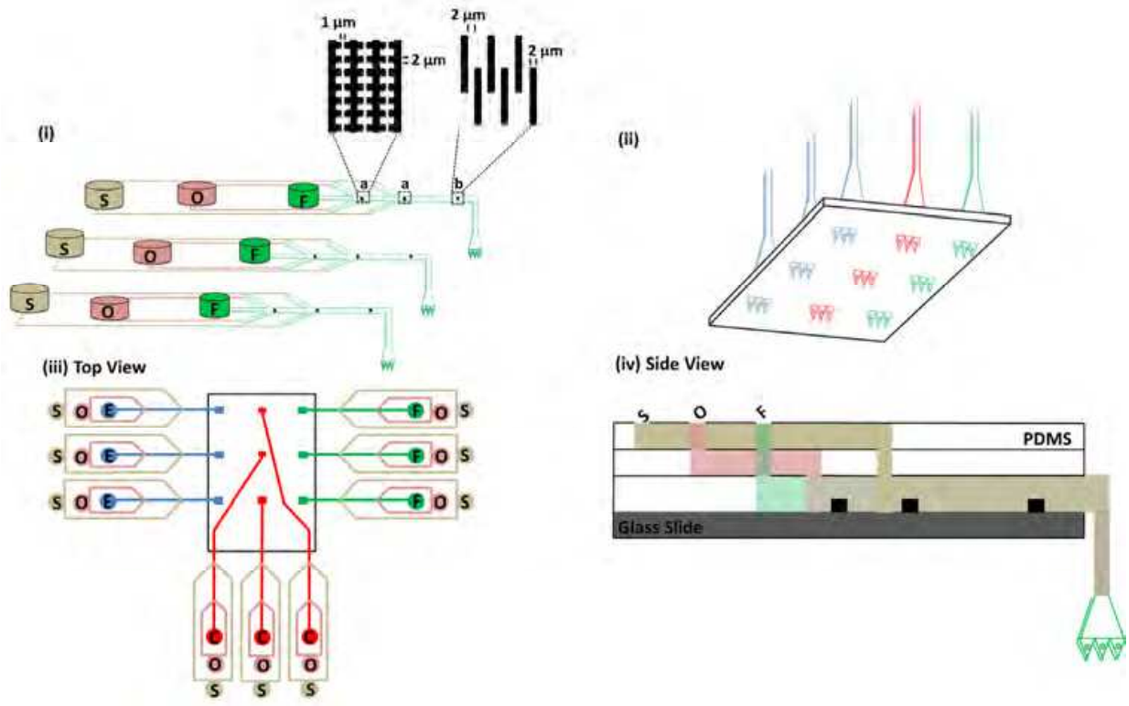


Fig. 2. Microfluidic drug delivery device for cancer treatment. (i) Overview of fluorouracil drug system including drug, oil and saline storage including (a) electrodispersion electrodes and (b) dielectrophoretic micropumping electrodes. Microchannel dimensions are 25 µm (width) x 25 µm (height). (ii) Termination of microchannels into the microneedle system. (iii) Top view of ECF droplet microdevice. And (iv) Side view of multilayered system for droplet dispersion and flow to the microneedles. The abbreviations are S = saline, O = poppy seed oil, F = fluorouracil, E = epirubicin, and C = cisplatin.

Chemotherapy is a common treatment option for gastric cancer. Several single chemotherapy drugs have been used to treat gastric cancer including 5-fluorouracil, mitomycin, doxorubicin, cisplatin, etoposide, docetexal, and methotrexate. Efficacy of these drugs are typically measured via clinical response rates, which is the percentage of patients that respond to cancer treatment such that cancer cells are no longer detected. The response rates to these drugs were poor ranging from 15-35% (Cleveland Clinic Foundation, 2010; Hershock, 2006; Levi et al., 1979). More effective treatments use a combination of two, three or more chemotherapy drugs. Combining two chemotherapy drugs has been examined by Levi et al. and response rates for drug cocktails increased to 40-50% (Levi et al., 1979). McDonald et al. combined three chemotherapy drugs fluorouracil, doxorubicin, and mitomycin and results showed a 55% response rate (Levi et al., 1979). Rivera et al. studied docetexal, a newer chemotherapy drug, in combination with cisplatin and 5-fluorouracil (DCF). DCF was compared with docetexal/cisplatin (DC) and cisplatin/5-fluorouracil (CF), and the objective response rates for DCF were 37-43%, 26% for DC, and 25% for CF. Based on these results it can be concluded that a combination of three chemotherapy drugs are more effective than two chemotherapy drugs (Rivera et al., 2007). Other combination chemotherapy drugs have been studied, and their response rates were: epirubicin, cisplatin and, 5-fluorouracil (ECF) 71%; 5-fluorouracil, adriamycin, and mitomycin 50% and 9%; 5-

fluorouracil, leucovorin, and cisplatin 44%; 5-fluorouracil, adriamycin, mitomycin, and methotrexate 42%; cisplatin, epirubicin, leucovorin, and 5-fluorouracil 43% docetexal, cisplatin, and 5-fluorouracil 37-43%; (Hershock, 2006; Power et al., 2010). Epirubicin, cisplatin, and 5-fluorouracil (ECF) had the highest response rate of 71%. In summary, response rate data suggests that combination chemotherapy drug treatment is the superior treatment option. Therefore, the microfluidic device described here will utilize the combination of ECF. In the device depicted in Figures 1 and 2 each individual drug in the ECF drug system is stored in separate reservoirs so their dosage can be independently controlled via feedback electronics. There is also redundancy in the microchannels and microneedles for backup in case any of the channels become clogged over time. Within the microchannels each drug is sheathed in a biocompatible oil in order to protect the integrity and enhance drug efficacy over the dosage cycle.

This chapter will further explore the integration of microchannels, electrodispersion, dielectrophoretic pumping, and microneedles in a dynamically controllable microfluidic platform to deliver ECF to gastric cancer patients.

## 2. Technologies utilized in the drug delivery microfluidic device

### 2.1 Microchannels and electrodispersion

Emulsions are mixed dispersions of more than two immiscible fluids via encapsulation of one layer by the other layer. These emulsion droplets are useful in areas such as foods, cosmetics, pharmaceutical drug delivery, and chemical synthesis. Examples of foods include milk, yogurt, sauce, butter, etc. and cosmetics of lotion (oil-in-water, O/W), cream (water-in-oil, W/O), hair, shaving, and bath products that are predominantly viscous liquids (Mezzenga, 2005; S.H. Kim et al., 2011). In chemical synthesis, droplets are being used as a new reaction platform due to their ability to function as a batch reactor such as antimicrobial agent and preservatives (Hamouda et al., 1999; Jensen & Lee, 2004; Mejia et al., 2009). The forms of emulsion droplets to contain various physical and chemical compositions are effective in delivering drugs and cosmetics in human body (Wibowo & Ng, 2001; Kiss et al., 2011).

In this drug delivery microfluidic device, flow focusing (FF) hydrodynamics and electrodispersion technology are combined to dynamically generate oil-sheathed drug droplets on the order of 100 nm outer diameter dispersed in saline. Poppy seed oil is used to decrease the toxicity of the chemotherapy drug (Pai et al., 2003) while maintaining its potency and efficacy once it reaches the target malignant cells, and saline is used to carry the droplets into the tissue during injection. Our drug delivery microdevice will combine both FF and electrodispersion technologies in order to achieve narrower size distribution of particles by preventing droplet interactions and coalescence. Electric fields are added for chemotherapy drug droplet formation to decrease the size of droplets, improve robustness of continuity of the droplet thread formed, and increase velocity as droplets travel downstream in the microchannel. Thus, the main focus of our study is developing FF geometry with electrodispersion and adequate use of surfactants to generate submicron droplets (~100 nm) with highly uniform sizes to promote a quick transport into cells.

Emulsion droplets of very narrow size distributions can be strategically generated by harnessing hydrodynamic behaviors within microfluidic systems (Anna et al., 2003; Martin-

Banderas et al., 2005; W. Lee et al., 2009). FF geometries are used in mixing immiscible phases or encapsulating one phase within a second sheathing phase. Typically, hydrophobic drops are dispersed in a hydrophilic fluid or vice versa. The drug delivery microdevice utilizes this technology in order to protect the inner fluid (drug) by an outer fluid (oil) which is then dispersed in a continuous saline stream. The inner phase is traditionally termed the dispersed phase while the outer phase is termed the continuous phase when they meet at an orifice. Most microfluidic emulsions involve a single droplet dispersed in a continuous phase such as water-in-oil (W/O) and oil-in-water (O/W) (Ha and Yang, 1999; Anna et al., 2003; W. Lee et al., 2009; Kiss et al., 2011). This concept can also be expanded to droplets that include more than one internal droplet such as double emulsions (W/O/W or O/W/O) (Utada et al., 2005; Seo et al; 2007; Liao and Su, 2010; S.H. Kim et al., 2011) and are the foundation for the drug delivery microdevice described in this chapter.

During small droplet synthesis, mechanical shear stress was utilized in order to achieve small and highly stable emulsion droplets, but this approach yielded tens of nano- to hundreds of micro-scale droplets with large size distributions, which was problematic (Pacek et al., 1999; Abismaïl et al., 1999). The key advantage of FF technique is precise control in producing droplets into the range of hundreds of nanometers (Anna et al., 2003; Thiele et al., 2010), but ambiguity remains regarding the lower limit of droplet sizes that can be achieved, the size distribution and continuity of the droplet threads still remain unreported due in part to the difficulty of in-line droplet size analysis and the length of the droplet thread (Anna et al., 2003; W. Lee et al., 2009). The goal in this drug delivery microdevice is to generate the smallest droplets possible because larger droplets are less stable and more likely to come in contact with each other which leads to droplet deformation and coalescence. Other studies have determined that 50-150 nm droplets ensure an optimal intake in cells for drug delivery applications (Thiele et al., 2010). In addition, larger droplets are less stable and more likely to come in contact with each other which leads to droplet deformation and coalescence.

Because the drug delivery microfluidic system dimensions are designed to fit within a wristwatch-like system on a human wrist, multilayered FF and electrodispersion are proposed for ECF chemotherapy drug emulsion and delivery, Figure 2(ii-iv). The total dimensions of multilayered ECF drug system is small enough to be non-obtrusive, so that it can be worn for continuous drug delivery with minimal discomfort as shown in Figure 1. In the drug delivery microdevice, two FF orifice/junction geometries are utilized in series as shown in Figure 3. The two junctions whereby sheathing flows of poppy seed oil and saline are added to the main channel are 3mm long, 20 μm wide, and 20 μm deep in the microchannel, and the continuous and dispersed phases are injected through pressure regulated membrane deflection into the fluid reservoirs which operate as micropumps. Such designs are also commercially available and meet the volume and portability limitations of the proposed wristwatch system, as well as the energy demand limitations (Lima et al., 2004). The flow rate inputs are 0.01 μL/min of drug, 0.1 μL/min for poppy seed oil, and 1 μL/min for saline based on the reduction of the optimal flow conditions achieved by Zagnoni et al., 2009 & 2010 to meet our channel dimensions in which the ratio of the continuous and dispersed phase flow rate are held at 10 to achieve submicron droplets in the downstream microchannels.

Achieving drug droplets with diameters at approximately 500 nm is feasible via the hydrodynamic flow focusing achieved with the 4 μm wide orifice and combined with the

strategic use of surfactant chemistry (W. Lee et al., 2009). Droplet size is determined initially by the orifice geometry; however, a surfactant mixed with either the continuous or dispersed phase balances interfacial tension and enables droplet sizes to be orders of magnitude smaller in comparison with those without a surfactant (W. Lee et al., 2009). That is, adding a proper surfactant can improve stability of the droplets and decrease the size of droplets because the surfactant molecules reduce the interfacial tension between different fluids in a droplet, thus avoiding the undesirable coalescence among droplets. For this chemotherapy drug delivery application, proper surfactant selection requires biocompatibility which must be considered as well as long-term drug-surfactant interactions. To avoid the later, surfactants will be dispersed in the oil phase and in the saline phase.

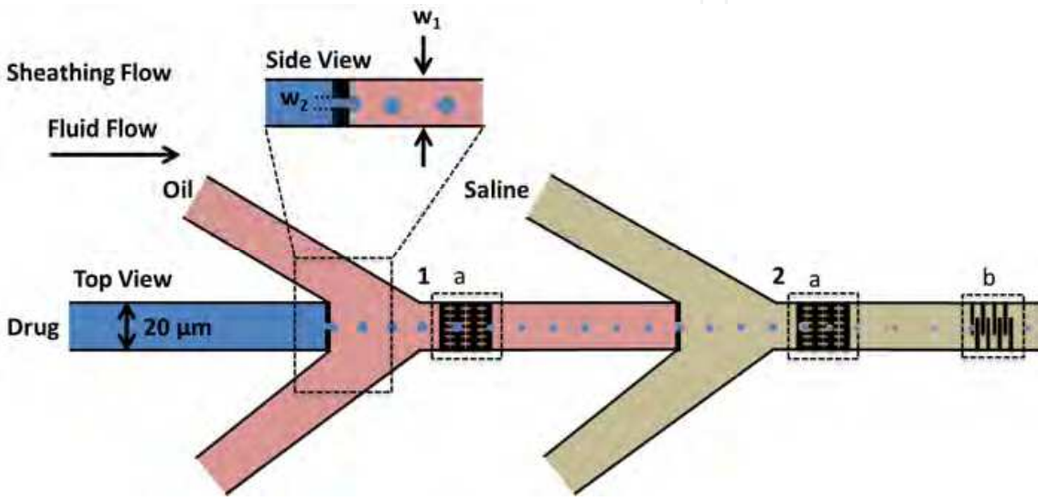


Fig. 3. Microchannel design for the chemotherapy drug emulsion formation with flow focusing and sheathing flow; appropriate scale not reflected. Dashed boxes (a) and (b) correspond to the placement of the electrodes for electrodispersion and dielectrophoretic micropumping, respectively. $w_2$ is the orifice depth 4 µm, and $w_1$ is the depth of the junction 20 µm . The aqueous drug solution flows through the microchannel until it is dispersed into the continuous oil phase at junction 1. At junction 1 orifice, drug-in-oil droplets are formed and flow until they are then dispersed into the saline phase at junction 2 to achieve an oil sheathing of the drug droplet in the continuous saline phase. Double emulsion chemotherapy droplet is produced via the second orifice. See Figure 4 for the COMSOL simulation of this fluid flow.

The droplet formation behavior is mainly determined by capillary number (Ca), which represents the balance between the viscous forces and interfacial tension at the surface of two fluids as defined in Equation 1. In Equation 1, µ is the viscosity of the continuous phase, V is the characteristic velocity, and γ is the surface tension. Capillary number is the most appropriate dimensionless number to describe droplet formation behavior because Reynolds number and Weber number are less significant in FF (W. Lee et al., 2009). In addition to Ca, the flow rate ratio (φ), the viscosity ratio (λ), and the expansion ratio (A) in Equations 2-4 (W. Lee et al., 2009) are also parameters to govern droplet formation because they balance viscous stresses and exerted shear stresses which result in droplet thread trajectory and velocity profile. In Equation 2, $Q_d$ and $Q_c$ are flow rate of dispersed phase and

continuous phase, respectively. In Equation 3, $\mu_d$ and $\mu_c$ are viscosity of dispersed phase and continuous phase and $w_1$ and $w_2$ are depth of outside and inside orifice.

$$Ca = \frac{\mu V}{\gamma} \tag{1}$$

$$\varphi = \frac{Q_d}{Q_c} \tag{2}$$

$$\lambda = \frac{\mu_d}{\mu_c} \tag{3}$$

$$\mathrm{A} = \frac{w_1}{w_2} \tag{4}$$

Accordingly, the size of droplets changes by capillary number due to viscous force and the interfacial tension. While flow rate ratio affects the droplet formation behavior significantly, the viscosity ratio has a relatively weak impact on the droplet diameter compared to capillary number (Ca) since the flow rate is associated with characteristic velocity of Ca. In addition, as the expansion ratio between the orifice and the junction depth decreases, a longer thread of smaller droplets is achieved, which is desired in the drug delivery microdevice. Much remains to be learned in regards to the underlying physics in the system as well as the stability of the droplet threads over long operation times. Therefore, a few assumptions were made in the FF designs of the microdevice. These assumptions include the combination of the FF droplet formation with the electrodispersion design to decrease droplet size, increases velocity of droplets, as well as with regards to the continuous robustness of producing droplets over long operation times (days) of the device.

Research has also been conducted in the related field of electrically manipulated emulsifications (H. Kim et al., 2007; Zagnoni et al., 2009; Zagnoni et al., 2010). Electric fields with a resonance frequency between 10Hz and 10MHz have been used as a separation method to remove water dispersed in oil for applications in the petroleum industry. This data is applicable to droplets in the drug delivery microdevice since the frequency-modulated electric field utilized can be used as a deformation tool for emulsion droplets (Zagnoni et al., 2009; Zagnoni et al., 2010). Electric fields have also been used to focus and space nano and micro emulsions/particles in microchannels of 50 μm (width)* 50 μm (length)* 61 μm (height) orifice dimensions in DC fields (H. Kim et al., 2007). H. Kim et al. studied electrospray emulsification and produced emulsion < 1 μm in diameter with ~2% of size distribution at a field of $1.4*10^2$ - $5.5*10^3$ V/m, and also Arya et al. successfully synthesized hundreds of nm chitosan micro/nano spheres for drug delivery application in $2.3*10^5$- $4.7*10^5$ V/m. Furthermore, Mejia et al. formed wax emulsions with high uniformity for water-proof painting, cosmetics, and adhesives that supports the idea of utilizing electric field (2.6-2.9 kV in 500 ml wax mixture) in the production of fine emulsions. Compared to these literature values of the applied electric fields, the device operating condition of $5*10^6$-$10^7$ V/m is several orders are higher.The electric energy acting on the particles cause the water-oil interface to charge such that it behaves as a capacitor, which leads to a tip of Taylor cone which enables tiny droplets and narrow size distribution ~2% (H. Kim et al., 2007).

Castellation configuration electrodes (Zagnoni et al., 2009; Zagnoni et al., 2010) were designed for electrodispersion because this design resulted in the highest localized electric field in the z-dimension which has the potential to most efficiently manipulate the droplets and minimize deformation in the x- and y- directions. These are placed 200 µm downstream from both junction 1 and junction 2 as shown in Figure 3 (a). This electric field energy does two things: a) it breaks apart the droplets from hundreds of nanometers in diameter into the more effectively adsorbed size of < 100 nm and b) it spatially disperses the droplets in the continuous phase in order to minimize coalescence as droplets travel forward in microchannel.

In order to simulate behaviors in the drug delivery microdevice, COMSOL 4.2 was used to simulate the 3D electric field gradient of the electrodispersion design in Figure 4, which is castellated gold electrodes of gap width 1 µm (x-direction), width 2 µm (y-direction), and thickness 20 nm (z-direction). The electrostatics module with the electrostatic potential (Equation 5), a relationship between electric displacement and the electric field (Equation 6), and Gauss's law (Equation 7) were used to simulate the electric field gradient in a fluid medium of saline.

$$\vec{E} = -\vec{\nabla} V \tag{5}$$

$$\vec{D} = \varepsilon_0 \vec{E} + \vec{P} \tag{6}$$

$$\vec{\nabla} \cdot \vec{E} = \frac{\rho_V}{\varepsilon_0} \tag{7}$$

In Equations 5-7, $\vec{E}$ is the electric field, V is the electric potential, $\vec{D}$ is the electric displacement, $\varepsilon_0$ is the permittivity of a vacuum, $\vec{P}$ is the electric polarization and was assumed to be zero in the fluid medium, and $\rho_V$ is the space charge density. Combining Equations 5-7 with zero electric polarization gives

$$\vec{\nabla} \cdot \left( \varepsilon_0 \varepsilon_r \vec{E} \right) = \rho_V \tag{8}$$

Equation 8 is the governing equation used in to simulate the electric field gradient of the electrodispersion electrode design (Figure 3). Equation 8 is modified slightly and employed in COMSOL as

$$\nabla E = \sqrt{\frac{\partial^2 E}{\partial x^2} + \frac{\partial^2 E}{\partial y^2} + \frac{\partial^2 E}{\partial z^2}} \tag{9}$$

In COMSOL, the physical properties for water were altered slightly to simulate the saline such as 8.9 x $10^{-4}$ Pa·s dynamic viscosity and 80 relative permittivity. The physical properties used for poppy seed oil were dynamic viscosity 5.58 x $10^{-2}$ Pa·s and relative permittivity of 4. Poppy seed oil is used to decrease the immediate toxicity of the chemotherapy drug (Pai et al., 2003) as it enters the tissue, and saline is used to carry the sheathed droplets and match tissue isotonicity during injection. Gold was the material used for the electrodes, and PDMS was the material used to form the orifices at the microchannel junctions (see Figure 2 for

orifice design) as reported in the literature (W. Lee et al., 2009). The initial flow rates in the microchannels were chosen to be 0.01 μL/min of drug, 0.1 μL/min for poppy seed oil, and 1 μL/min for saline. These initial flow rate values were chosen based on Zagnoni et al. 2009 and 2010.

The fluid flow velocity in the FF microchannel was modeled with the laminar flow module employing the Navier Stokes equation and the continuity equation, which were simplified by assuming a steady-state system and an incompressible fluid as follows:

$$\rho(v \cdot \nabla)v = -\nabla p + \nabla\left(\mu\left(\nabla v + \nabla^T v\right)\right) + F_S \tag{10}$$

$$\nabla \cdot v = 0 \tag{11}$$

In Equations 10 and 11, ρ is the fluid density, v is the fluid velocity, t is time, p is the pressure, μ is the viscosity, and $F_S$ is the volumetric force on the fluid resulting from surface tension.

Two types of fluidic conditions of water (to represent drug and saline) and oil were employed, and the velocity of the formed emulsion droplets were calculated from the summation of pressure driven flow velocity and electro-osmotic velocity. The electro-osmotic flow velocity was calculated from Smoluchowski slip velocity equation via a wall boundary condition on the microchannel and added to simulate the velocity of the chemotherapy droplets in the field created by the electrodispersion, Figure 3. The zeta potential for PDMS was assumed at -0.1V (Kirby and Hasselbrink Jr., 2004). The boundary condition for electrical potential was an applied DC field of 10V and ground across each pair of electrodes. The velocities without electrodes were calculated from pressure driven flow in the x-, y-, and z-direction and expressed with $u_i$. The governing equations for electro-osmotic flow used for this simulation are Equation 12-16 below,

$$\mu_E = \frac{\varepsilon_r \varepsilon_0 \zeta}{\eta} \tag{12}$$

$$v_{EOF,i} = \mu_E \cdot \vec{E}_i \quad \text{where i = x,y,z} \tag{13}$$

In Equations 12 and 13, μE is electrophoretic force, $\varepsilon_r$ is the relative permittivity of the fluid, $\varepsilon_0$ is the permittivity of a vacuum, ζ is the zeta potential, η is the dynamic viscosity, $v_{EOF,i}$ is the velocity due to electro-osmotic flow (EOF), and $\vec{E}$ is the electric field. The normal EOF velocity and the total velocity of the droplets are given as

$$v_{norm} = \sqrt{v_{EOF,x}^2 + v_{EOF,y}^2 + v_{EOF,z}^2} \tag{14}$$

$$v_{total} = \sqrt{v_{x,total}^2 + v_{y,total}^2 + v_{z,total}^2} \tag{15}$$

The EOF velocity is related to the total velocity by

$$v_{i,total} = u_i + v_{EOF,i}^2 \quad \text{where i = x,y,z} \tag{16}$$

The total velocity is displayed in the simulation scale bar next to each COMSOL diagram in Figures 4 and 5.

Figure 4 shows the electric field gradient with and without the droplets. The maximum electric field gradient without droplets is 1.1 x $10^7$ V/m and the maximum electric field gradient with droplets is 2.3 x $10^7$ V/m. This difference is because when the droplets pass in between the two electrodes, the droplets have an induced field which influences the applied field gradient by reducing the gap over which the potential acts. The electric field is tuned to the resonant frequency of the droplets in order to break apart the ~500 nm droplets into < 100 nm droplets as well as distribute the droplets spatially within the continuous fluid phase.

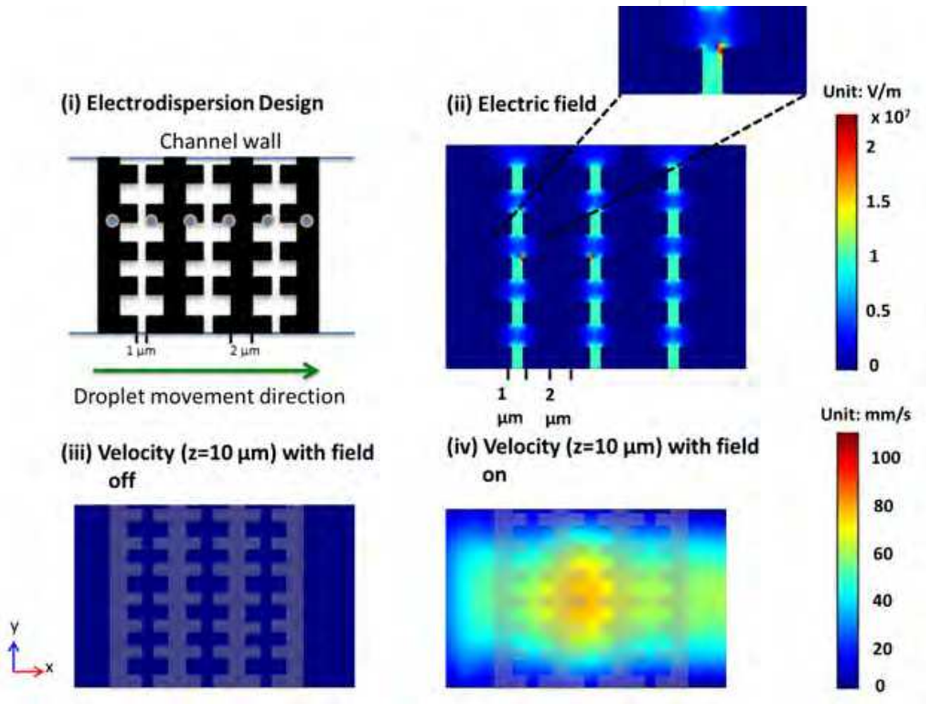


Fig. 4. COMSOL simulations of the electric field gradient as well as the velocity profiles (without and with the E field active) at the midpoint (x, y plane at z = 10 µm height) of the microchannel. (i) Channel level view of electrodes with cartooned drug droplets, (ii) electric field magnitude, (iii) fluid velocity above the inactivated electrodispersion electrodes at junction 1 (roughly 0.056 mm/s), and (iv) fluid velocity once the electric field is activated (maximum velocity roughly 73.0 mm/s). The maximum observed electric field strength during fluid flow is 2.3 x $10^7$ V/m.

The drug delivery microdevice is designed so that it can be easily fabricated with standard UV-photolithographic methods in a Class 100 or greater cleanroom. The FF geometry integrated within the microchannel design is fabricated in poly (dimethylsiloxane) (PDMS) using standard printed masks, UV soft photolithography techniques, and multilayer alignment of the channels from one layer to the next. The electrodes can be fabricated on a silicon or glass support via photoresist masking followed by deposition of a 10 nm titanium layer then a 10 nm gold layer by electron-beam evaporation.

Each layer of the molded channels can be sealed via oxygen plasma bonding procedures. PDMS is hydrophobic so that oil wets the walls, but surface treatment defines the required hydrophobic and hydrophilic patterns depending on fluid phases used. The dispersed drug phases will be hydrophilic (viscosity, $\mu_c$= 6 mPa·s) and a biocompatible surfactant will be mixed with either the continuous phase or the dispersed phase at a concentration approximately 2.5 times greater than the critical micelle concentration (CMC) which is a moderate surfactant concentration and is favorable to test a wide flow rate range (W. Lee et al., 2009). The presence of the surfactant does not substantially change the viscosity as evidenced by W. Lee et al.

A positive displacement chamber pump connected across a membrane to a pressurized canister will be used to drive the fluids from each inlet into the FF microchannels. Separate micropumps will connect to each solution reservoir such that flow in each channel can be separately controlled to achieve a feedback controlled fluidic system that can be worn on a wrist (Lima et al., 2004). Pressure drops for flows between 0.01 and 1 μL/min are not expected to cause deformation of microchannels due to either high-pressure injection or the PDMS elasticity used in our drug microdevice (Soller et al., 2011). If necessary, Thermoset Polyester (TPE) would be the best alternative material of PDMS due to its high rigidity and suitability with droplet microfluidics (Soller et al., 2011).

In order for a stable, efficient, and continuous small dosage of drug delivery, optimized selection of a surfactant, microfabrication condition, and pumping system are discussed. The unique combination of FF and electrodispersion to generate drug droplets protected by a sheathing layer of biocompatible poppy seed oil is described. Further, the electric field and fluid flow conditions were simulated and results are used to optimize the design. The droplets exiting the FF and electrodispersion region must then be accelerated in the drug delivery microdevice channel in order to generate a high enough pressure difference for the fluid to exit the microneedles into the dermis of the skin to achieve drug delivery.

### 2.2 Dielectrophoretic pumping

Traveling wave DEP (twDEP) is incorporated into the drug delivery microdevice in order to accelerate the chemotherapy droplets as they travel to an array of microneedles for painless injection into the body. DEP is an efficient nondestructive way to manipulate bioparticles (Cheng et al., 2011), and twDEP is being investigated as a possible drug delivery technique (Bunthawin et al., 2010). The electrode configuration consists of an array of parallel rectangular electrodes configured in an intercalated pattern as shown in Figure 1(ib). The intercalated configuration of the electrodes facilitates horizontal movement of particles when a non-uniform AC field is applied that is offset by 90° with each successive electrode. This causes the field maxima to travel in waves down the array of electrodes thus driving the particle forward. Typically the spacing between the electrodes is fixed to the width of one single electrode with the optimal width of an electrode being close to the diameter of the target particle. The spacing between the electrodes is usually 10 μm to 50 μm and remains constant (Lin & Yeow, 2007).

Parallel electrodes are used for collecting, transporting, and/or separating particles. For the drug delivery microdevice, we will be using the parallel electrodes for transporting the oil-sheathed chemotherapy droplets. To help facilitate transportation the frequency and

conductivity of medium is chosen specifically to induce the largest positive DEP force on the dielectric particles. Positive DEP is the movement of particles up the electric field gradient. When the AC field is applied to the electrodes a dipole moment is induced in the particles and the time-average DEP force, $<F_{DEP}>$, is given as (Pethig, 2010)

$$\left\langle F_{DEP} \right\rangle = 2\pi\varepsilon_m R^3 \left\{ \mathrm{Re}\left[f_{cm}\right]\nabla E^2 + \mathrm{Im}\left[f_{cm}\right]\sum E^2\nabla\phi \right\} \tag{17}$$

In Equation 17 $\varepsilon_m$ is the absolute permittivity of the medium, R is the radius of the particle, $f_{cm}$ is the Clausis-Mossotti factor, E is the amplitude of the electric field, and $\phi$ is the phase. The Clausius-Mossotti factor is related to the polarizability of the particle and $\sum E^2\nabla\phi$, is the summation of the magnitude and phase of each field component. The Clausis-Mossotti factor, $f_{cm}$, for a spherical, homogeneous particle is given as (Pethig, 2010)

$$f_{cm} = \frac{\underline{\varepsilon}_p - \underline{\varepsilon}_m}{\underline{\varepsilon}_p + 2\underline{\varepsilon}_m} \tag{18}$$

In Equation 18 $\underline{\varepsilon}_p$ is the complex permittivity of the particle and $\underline{\varepsilon}_m$ is the complex permittivity of the medium defined as (Pethig, 2010)

$$\underline{\varepsilon}_p = \varepsilon_p + \frac{\sigma_p}{j\omega} \tag{19}$$

$$\underline{\varepsilon}_m = \varepsilon_m + \frac{\sigma_m}{j\omega} \tag{20}$$

In Equation 19 and 20 $\varepsilon_p$ is the absolute permittivity of the particle, $\sigma_p$ is the conductivity of the particle, $\sigma_m$ is the conductivity of the medium, $\omega$ is the angular frequency and j is the imaginary number. It is important to note that the DEP force for twDEP is dependent on both the real and imaginary part of the Clausius-Mossotti factor which causes particles to experience both an in-phase force (real part) and the out of phase force (imaginary part). Classical DEP force is only dependent on the real portion of the Clausius-Mossotti factor, $\left\langle F_{DEP} \right\rangle = 2\pi\varepsilon_m R^3 \,\mathrm{Re}\left[f_{cm}\right]\nabla\left|E\right|^2$.

Further, the assumption that the oil-sheathed droplets of aqueous drug can be represented as a first approximation homogeneous particle is acceptable because the conductivity of the oil layer is substantially different (≈ 1 nS/m) from the supporting saline medium that the Clausius-Mossotti factor is nearly 0.50 – 3.36*10$^{-8}$i and varies very little (< 0.01%) over the anticipated frequency range of interest from 1 Hz to 10 MHz (Durr et al., 2003; Felten et al., 2008). Since twDEP is being used to transport chemotherapy droplets, it's important to have an expression that relates the particle electrophoretic mobility with twDEP force. The DEP force can also be written utilizing the zeta potential $\zeta_p$ (Kang & Li, 2009),

$$\vec{F}_{DEP} = 6\pi\zeta_p\varepsilon_r RE \tag{21}$$

The DEP force written in this form allows it to be related to the electrophoretic mobility of the particle given as (Kang & Li, 2009)

$$\mu_E = \frac{\varepsilon_r \varepsilon_0 \zeta_p}{\eta} \tag{22}$$

$$v_{DEP} = \frac{R^2 \varepsilon_r \varepsilon_0 \,\mathrm{Re}\left[f_{cm}\right]}{3\eta} \nabla E \tag{23}$$

In equations 21-23 $\zeta_p$ is the zeta potential, $\varepsilon_r$ is the relative permittivity of the medium, R is the radius of the particle, E is the magnitude of the electric potential, $\varepsilon_0$ is the permittivity of free space, Re[$f_{cm}$] is the real-part of the Clausis-Mossotti factor, and $\eta$ is the dynamic viscosity of the medium.

Parallel electrodes were added to the end of the microchannels, Figure 2(ib), to increase the velocity of the chemotherapy droplets to ensure the droplets reach the microneedles at the end of the device with sufficient velocity to penetrate the dermis. The desired velocity at the microneedle tips was 10 μm/s based on modeling of transdermal delivery (Lv et al., 2006). COMSOL was used to simulate the electric field gradient via the conservation of electrical potential between the insulating channel walls and the velocity of the droplets via the Navier-Stokes (Equation 12) and conservation relationships (Equation 13). Equations 5-9 developed in section 2.1 were used to obtain the electric field gradient with and without droplets in the channel as shown in Figure 5. Droplets were defined as separate spherical

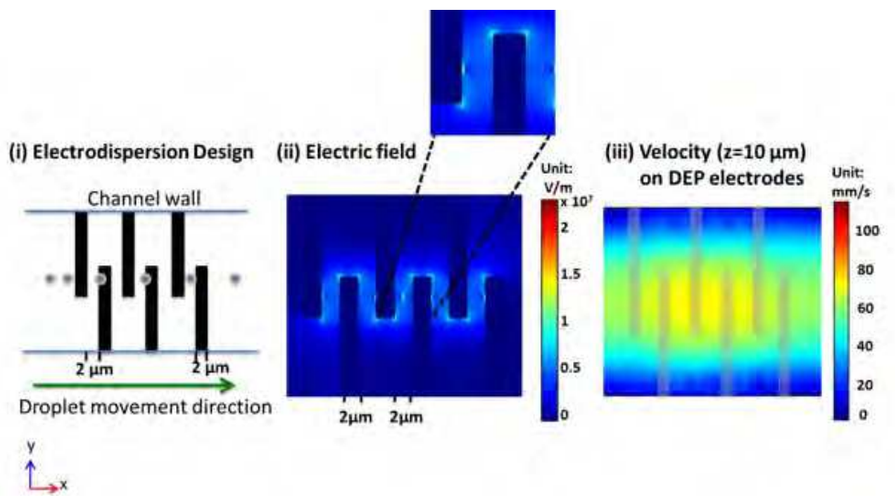


Fig. 5. COMSOL simulation of traveling wave dielectrophoretic pumping electrodes before and during fluid flow in the microchannel. The combined total length of the electrodes including gaps is 22 μm (i) channel level view of electrodes, (ii) normalized electric field strength from twDEP electrodes, (iii) velocity distribution in the channel view. In (i) when the twDEP electrodes are energized at an instantaneous half cycle with max potential of 10Vpp to ground at subsequent electrodes. The maximum observed electric field strength before fluid flow is 7.2 x $10^6$ V/m, and the maximum electric field strength during fluid flow is 1.1 x $10^7$ V/m. The droplet fluid maximum velocity was 73 mm/s in this DEP pumping region at z = 10 μm.

fluids with the laminar flow module in COMSOL. The material selected in COMSOL for the particles was oil as previously described in section 2.1 and modified water to represent saline. It can be seen in Figure 5 that the electric field gradient decreases by 65% when the droplets are present because of the change in the electric charge of the dielectric oil layer. Further, the droplets align along the centerline of the electrode configuration because the DEP force is directed toward the symmetric centerline. This phenomenon is observed because electric field interact with droplets and induce force due to the dielectric property difference between immiscible phases (water and oil) since free charges can accumulate on the interface between inner and outer fluid. The behavior of the droplet velocity was examined in z-dimension revealing that the electric field primarily affects the velocity of the droplets near the electrodes ($z < 3\text{-}4\mu m$). The droplet equilibrium height is 10 microns above the bottom of the channel. DEP forces are predicted to be on the order of 152 pN for the 10 Vpp field over the 22 μm electrodes.

The electrophoretic mobility was used to simulate the velocity of the chemotherapy droplets in the field created by the dielectrophoretic pumping electrodes. In this drug delivery microdevice system, the droplet is a chemotherapy drug coated with poppy seed oil in a continuous phase of saline. In order to look at electric field effect, electrophoretic mobility was an added term.

In Figure 5, the local fluid velocities increased by over 5000 times from 0.021mm/s to 109 mm/s by implementing dielectrophoretic pumping at 10 Vpp via the electrode designs in the COMSOL simulation. Comparing without and with dielectrophoretic pumping (Figure 4(iv) and Figure 5(iii), respectively), the velocities with electrodispersion and DEP pumping electrodes remarkably changed as demonstrated in Figure 6. These increases in velocity are necessary to move the drug droplets forward to the microneedles for injection.

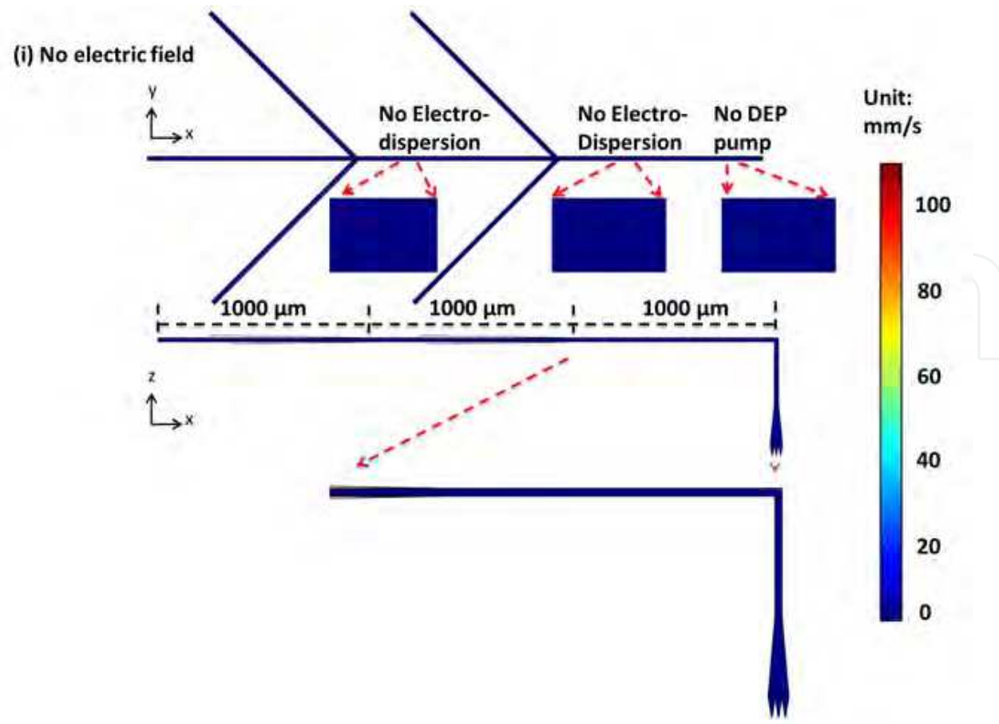

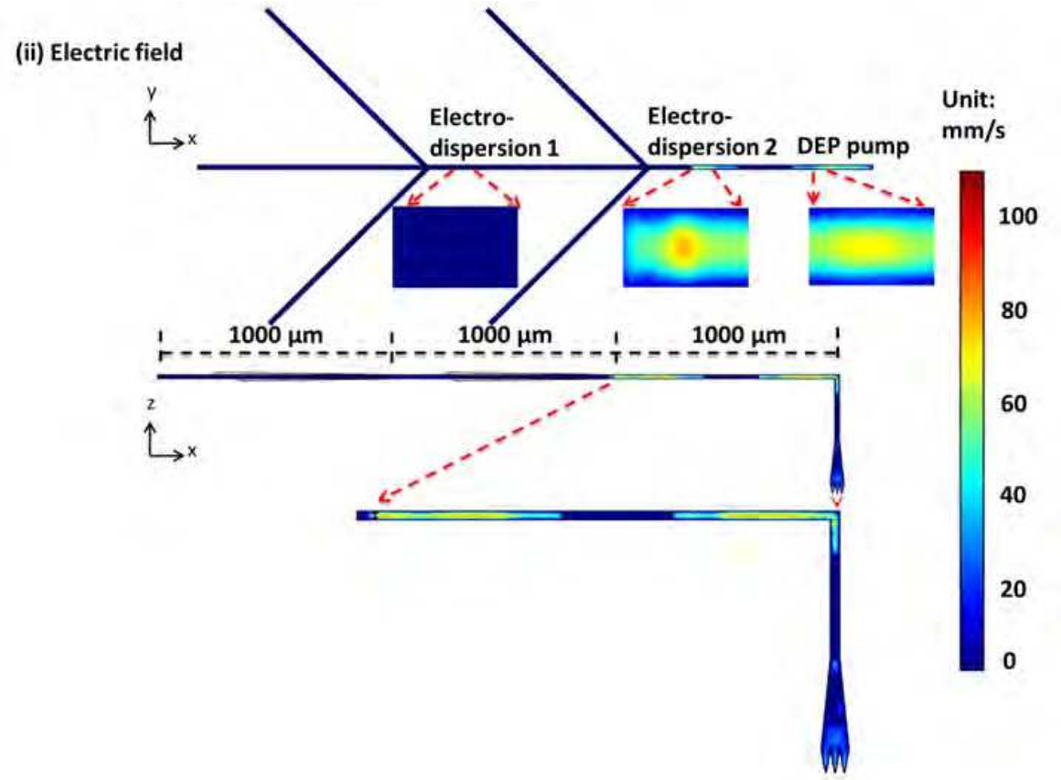


Fig. 6. The top of each simulation shows x-y plane, top view, and bottom of each simulations shows z-x plane to display overall velocity profile. COMSOL simulation of fluid velocity without (i) and with (ii) dielectrophoretic pumping electrodes. Interdigitated dielectrophoretic pumping electrodes were added to the end of the microchannel to increase the velocity of the chemotherapy drug droplets to ensure sufficient velocity for microneedle injection. (i) The maximum fluid velocity inside the microchannel without electrodes was 0.025 mm/s reached at junction 2, (ii) the maximum fluid velocity with electrodes was 109 mm/s also at junction 2. The magnified sections for (i) and (ii) show that the fluid velocity substantially increases from 0.0056 mm/s to 35 mm/s at the end of the microchannel once the pumping electrodes are added.

### 2.3 Microneedles

The skin is a common area for drug delivery, and offers advantages over other non-invasive drug delivery techniques. Drug delivery through the skin avoids drug metabolism by enzymatic reactions and the gastro-intestinal, has the potential for continuous drug delivery (Migalska et al., 2011), and facilitates reaching circulating tumor cells (CTCs) that metastacized from their origin. Hypodermic needles are commonly used as the dominant method for transdermal drug delivery for gastric cancer treatment. Needles are painful, inconvenient and require professional administration for each dose (P.M. Wang et al., 2006). Another problem is that drugs are delivered all at once which causes an immediate spike in drug concentration profiles which then rapidly diminishes. This can cause physiological instabilities, other dosage-related side-effects and can potentially fail to completely eradicate the tumor and/or CTCs (Zahn et al., 2004). To overcome these drawbacks, this work

proposes a novel drug delivery microdevice amenable to feedback control; the device integrates microchannel hydrodynamic flow focusing, electrodispersion to decrease drug droplet size, dielectrophoretic pumping, and microneedles together in one microdevice to deliver chemotherapy drugs in the form of droplets to a gastric cancer patient.

The skin has four layers: (1) the stratum corneum, principal barrier composed of corneocytes, (2) epidermis, (3) dermis, and (4) subcutaneous tissue (Escobar-Chavez et al., 2011). The four layers of the skin are barriers to transdermal drug delivery and microneedles are used as physical enhancers for transdermal drug delivery. They are designed to increase the permeability of the skin up to four orders of magnitude, so that drug passage through the stratum corneum and outer most layer of the epidermis becomes simple (Escobar-Chavez et al., 2011; K. Lee et al., 2011). Microneedles allow for drugs to be delivered across the skin in four ways: (1) "poke-with-patch", this method uses a solid microneedle array to penetrate the skin creating micropores, the microneedle array is removed and drugs are delivered through the micropores via a transdermal patch, gel or solution; (2) "coat-and-poke", this method coats an array of microneedles with a drug and inserts the coated microneedles into the skin; (3) "poke-and-release" embeds the drug molecules into the structure of polymer biodegradable microneedles and inserts them into the skin; and (4) "poke-and-flow", uses hollow microneedles to insert liquid drugs into the skin (Migalska et al., 2011). There are advantages and disadvantages to each approach and these vary with the application. Micropores created by microneedle penetration last for more than a day when left covered and they last for less than 2 hours when left uncovered. Microneedles that dissolve under the skin are perceived as the safest with the least chance of prolonged irritation (K. Lee et al., 2011). Methods 1, 2, and 3 are best suited for applications where a one time dose or daily dose of drug is desired. However, for the chemotherapy drug delivery microdevice, method 4 is optimal. The microneedles would remain inserted in the skin and held in place via a wristband as shown in Figure 1.

Microneedles can be inserted into the skin easier than hypodermic needles because stress on the skin is inversely proportional to the area of the top (Zahn et al., 2004). Microneedles require sharpness to overcome stress forces on the skin surface as well as strength against fracturing, bending, and buckling, sufficient flow rate, and biocompatibility of the needle material (Nguyen & Wereley, 2006). The insertion force can be lowered by utilizing kinetic energy such as vibration which can reduce the force by as much as 30% (Nguyen & Wereley, 2006), and provides an increase in infusion flow rate (P.M. Wang et al., 2006). Retracting the microneedles after insertion by approximately 100-300 μm also achieves a much greater flow rate (P.M. Wang et al., 2006).

Microneedles have been shown to increase the transdermal delivery of many molecules including aminovulinic acid, anthrax, bovine serum albumin, desmospressin, erythropoirtin, meso-tera(N-methyl-4-pyridyl)porphine tetra tosylate, ovalbumin, plasmid DNA, low molecular weight tracers to proteins, and nanoparticles. Insulin is the most widely studied drug with microneedles and enhanced skin permeability has been reported in vivo and in vitro (Donnelly et al., 2011; Escobar-Chavez et al., 2011). Recently researchers have looked into using microneedles fabricated from maltose to deliver methotrexate to rats via iontophoresis to treat cancer. The result of this study was a synergistic 25-fold increase of drug delivery (Escobar-Chavez et al., 2011).

Microneedles are a painless drug delivery method and create larger transport pathways for larger molecules; our device extends this to nanometer droplets. The painless characteristics of microneedles allow them to overcome the limitation of hypodermic needles. Advantages of microneedle technology are that the transport mechanisms are not dependent on the diffusion into the tissue, placement in the epidermis allows for drugs to reach target areas more readily, while only penetrating the stratum corneum without piercing nerve endings thus reducing pain, infection, or other injury. The microneedles are nontoxic, minimally invasive, can be mass-produced for a range of materials such as silicon dioxide and polymers, are easily disposable/interchangeable, and can be made from biodegradable materials. Some disadvantages to using microneedles are local inflammation and skin irritation. Another disadvantage is that the microneedles may break and be left under the skin; to avoid this, the diameter of the microneedle should be smaller than the diameter of a hair, ≤ 50 μm (Escobar-Chavez et al., 2011). In comparison hypodermic needles are inconvenient, not easily self-administered, and have poor targeted delivery because they have to be manually injected (P.M. Wang et al., 2006).

Our microdevice uses an array of microneedles, Figure 7, to deliver drug-in-oil microdroplets, applying the "poke-and-flow" method. Figure 7(i) shows the design of a single microneedle wherein the diameter of hole in the microneedles is approximately 40 μm which is sufficiently large to allow delivery of the oil sheathed drug droplets without disruptive shearing effects while simultaneously being large enough to avoid breakage in the skin. Figure 7(ii) is color coded to show the array of microneedles for each of the chemotherapy drugs with blue representing epirubicin, red representing cisplatin, and green representing fluorouracil. Each microneedle is connected to its own FF channel as shown in Figure 2. Figure 7(iii) shows a photograph of an array of microneedles (Baek et al., 2011) fabricated from polylactic acid. The fluid emulsion velocities are approximately 35 mm/s as they leave the DEP pumping electrode region. Once the emulsions enter their final descent, to the microneedles the midchannel linear velocity decreases to approximately 30 to 40 mm/s as the channel expands followed by velocity increases within the microneedle tip, as constrained by the continuity equation.

Several methods are used to fabricate hollow microneedles and most are made from silicon or silicon-based materials. This drug delivery microdevice requires a relatively straight channel with minimal bends so that the microdroplets are not sheared and are delivered to the dermis intact. The pyramid-shaped microneedles were chosen because fabrication is simple and thus it has the best shape to achieve tip sharpness and strength (Moon & Lee, 2003). The pyramid microneedles can be fabricated by an inclined LIGA process combining lithography, electroplating, and molding techniques. This process utilizes X-ray's directed towards a protective electroplated gold mask over a poly(methyl methacrylate) (PMMA) substrate on a silicon wafer (Moon & Lee, 2003).

As discussed in this section, optimal material, design, and operating conditions were gleaned from the literature. This information was combined to simulate electric field and hydrodynamic flow behaviors in each section of the microdevice. The design was iteratively optimized based on these simulation results and then integrated together into the drug delivery microdevice.

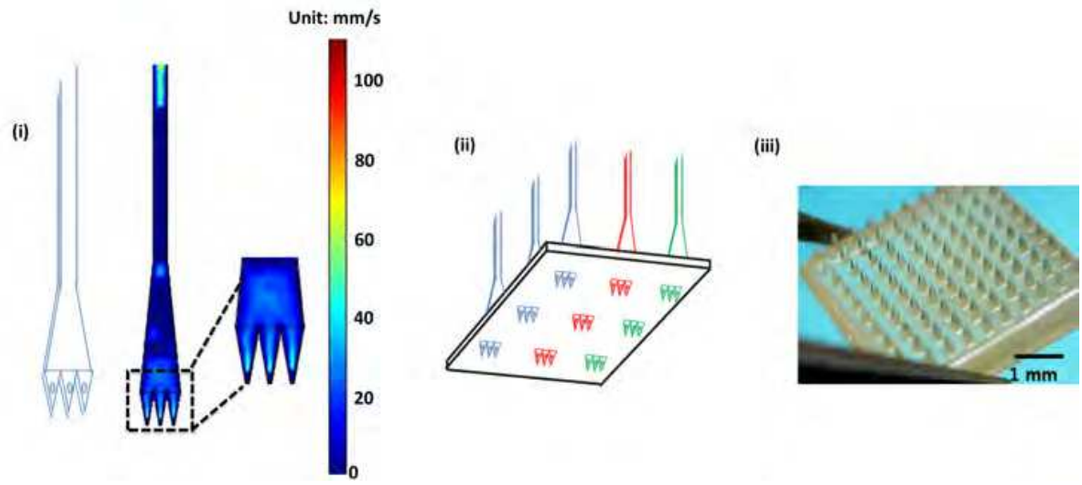


Fig. 7. Microneedle design to deliver chemotherapy emulsion to cancer patient, (i) pyramid-shaped hollow microneedle for delivery of 3 chemotherapy droplets (epirubicin, cisplatin, and fluorouracil) and the COMSOL simulation of the fluid velocity in the microneedle, (ii) microneedle array, and (iii) real image of a microneedle array. The initial velocities of the fluids in the microchannel were $4.2*10^{-4}$ m/s drug, $4.2*10^{-3}$ m/s poppy seed oil, and $4.2*10^{-2}$ m/s saline, and the exiting velocities from the microneedles is approximately 40mm/s. In (iii) microneedles are made out of poly-lactic acid (Baek et al., 2011).

## 3. Integration of technology into fully conceived device

This microfluidic drug delivery device will operate in sequence as described in sections 2.1 through 2.3. First, three different chemotherapy drugs, Epirubicin, Cisplatin, and Fluorouracil, will be separately dispersed into oil and then subsequently into saline by proven flow-focusing microchannel technology. Current state of the art results in this field suggest droplets formed will be approximately 500 nm in diameter. This design utilizes two stages of interdigitated electrodes on the bottom surface of the microchannel leaving the flow focusing junction in order to electrodisperse the droplets into <100nm droplets and to evenly disperse them spatially as they flow downstream to reduce coalescence. The oil-sheathed drug droplets are then pumped down the microchannel using traveling wave DEP technologies before flowing into an array of microneedles inserted into the dermis layer of the skin. This entire system is packaged inside of a small unit that can be worn on the wrist. The reservoirs for each drug, poppy seed oil, saline, and pressurized air to pump from the reservoirs can be individually replaced based on usage. Further, integrated electronic feedback control and monitoring (not described here) can be utilized to monitor chemotherapy drug delivery into the dermis and subsequently the blood stream of a cancer patient. The main components of this microfluidic device were optimized from literature data and COMSOL simulations.

## 4. Conclusions and perspectives for future integrated microdevice technologies

There is a great need for new technologies to effectively treat all forms of metastasized cancer. Gastric cancer provides a poignant example because patient symptoms typically do

not arise until the cancer has progressed to stage IV. Any new technologies developed should increase the comfort level of patients as well as concurrently improve treatment efficacy or even eradicate the disease. The goal of this work was to develop a novel drug delivery system to effectively treat gastric cancer patients with minimal pain or lifestyle interruptions while undergoing treatment.

In addition, this work links together technologies that have been progressing in isolation from each other. For example, electrodispersion integrated with flow focusing and surfactant stabilization is a novel technique with the potential to produce droplets less than 100 nm in diameter. Smaller droplets are desired in diverse applications such as nanoparticle synthesis or pharmaceutical packaging. One key advantage of this combined technique is that it can be integrated into lab-on-a-chip devices provided the capillary number and volumetric flow rate ratio which are optimized and the surfactant required for optimizing interfacial tension increases the long-term stability of droplets.

Traveling wave DEP is an advantageous technique for transport of droplets in microchannels, which has minimal power requirements and thus is ideal for portable microdevices operating on batteries. Incorporating traveling wave DEP electrodes into the drug delivery microdevice described increased the velocity of the droplets for optimal microneedle injection rates. Further, this technique has proven to be minimally disruptive to a particle which is a key advantage with this adaption of the technology in the drug delivery microdevice.

Microneedles have been explored in many forms as physical enhancers for drug delivery. Within the drug delivery microdevice, the microneedle array was adopted to reduce pain and facilitate continuous delivery of the Epirubicin, Cisplatin, and Fluorouracil chemotherapy drug cocktail into the dermis. Based on evidence from previous studies, the pain level can be greatly reduced and the chemotherapy droplets reach their target areas in a more efficient manner thus reducing side effects.

For future work this drug delivery microdevice wrist system could be improved by incorporating a biosensor, in-line feedback control, and wireless reporting to measure the concentration and metabolites of the chemotherapy droplets in the blood stream, dynamically adjust dosage, and keep the primary care physician informed of progress. This will allow for real-time drug and treatment monitoring. The advantages of adding in this technology would be decreases in patient drug side effects, uniform maintenance of the critical drug concentration delivered to the gastric tumor and CTCs, increased treatment effectiveness, and increased patient comfort.

## 5. References

Abismaïl, B., Canselier, J.P., Wilheml, A.M., Delmas, H., & Gourdon, C. (1999). Emulsification by ultrasound: drop size distribution and stability. *Ultrasonics Sonochemistry,* 6, 1-2, (March 1999), pp.75–83, ISSN 1350-4177.

Aboud, M.J., Gassmann, M., & McCord, B.R. (2010). The development of mini pentameric STR loci for rapid analysis of forensic DNA samples on microfluidic system. *Electrophoresis*, 31, 15, (August 2010), pp. 2672-2679, ISSN 0173-0835.

Alazzam, A., Stiharu, I., Bhat, R., & Meguerditchian, A. (2011). Interdigitated comb-like electrodes for continuous separation of malignant cells from blood using dielectrophoresis. *Electrophoresis*, 32, 11, (June 2011), pp. 1327-1336, ISSN 0173-0835.

American Cancer Society. (n.d.). Cancer facts & Figures 2012, In: *Cancer.Org*, August 2011, Available from: <http://www.cancer.org/Research/CancerFactsFigures/CancerFactsFigures/cancer-facts-figures-2011>.

Anna, S.L., Bontoux, N., & Stone, H.A. (2003). Formation of dispersions using "flow focusing" in microchannels. *Applied Physics Letters*, 82, 3, (January 2003), pp. 364-366, ISSN 0003-6951.

Arya, N., Chakraborty, S., Dube, N., & Katti, D.S. (2009). Electrospraying: A Facile Technique for Synthesis of Chitosan-Based Micro/Nanopsheres for Drug Delivery Applications. *Journal of Biomedical Materials Research Part B: Applied Biomaterials*, 88B, 1, (January 2009), pp. 17-31, ISSN: 1552-4973.

Baek, C., Han, M., Min, J., Prausnitz, M.R., Park, J.H., & Park, J.H. (2011). Local transdermal delivery of phenylephrine to the anal sphincter muscle using microneedles. *Journal of Controlled Release*, 154, 2, (September 2011), pp. 138-147, ISSN 0168-3659.

Reprinted from Journal of Controlled Release, 154, Baek, C., Han, M., Min, J., Prausnitz, M.R., Park, J.H., & Park, J.H., Local transdermal delivery of phenylephrine to the anal sphincter muscle using microneedles, pp. 138-147, Copyright (2011), with permission from Elsevier.

Balcer-Kubiczek, E.K., & Garofalo, M.C. (2009). Molecular targets in gastric cancer and apoptosis, In: Apoptosis in Carcinogenesis and Chemotherapy, Chen, C.G. and Lai, P.B.S., pp. 157- 192, Springer Science + Business Media, Retrieved from <http://www.crcnetbase.com/search/advanced>.

Bienvenue, J.M., Duncalf, N., Marchiarullo, D., Ferrance, J.P., & Landers, J.P. (2006). Microchip-based cell lysis and DNA extraction from sperm cells for application to forensic analysis. *Journal of Forensic Sciences*, 51, 2, (March 2006), pp. 266-273, ISSN 0022-1198.

Bjerklie, D. & Jaroff, L. (January 15, 2001). Beyond needles and pills, In: Time Magazine U.S., October 2011, Available from: < http://www.time.com/time/magazine/article/0,9171,998968,00.html>.

Brammer, K.S., Choi, C., Oh, S., Cobb, C.J., Connelly, L.S., Loya, M., Kong, S.D., & Jin, S. et al. 2009. Antibiofouling, sustained antibiotic release by Si nanowire templates. Nano Letters, 9, 10, (October2009), pp. 3570-3574, ISSN 1530-6984.

Bunthawin, S., Wanichapichart, P., Tuantranont, A., & Coster, H.G.L. (2010). Dielectrophoretic spectra of translational velocity and critical frequency for a spheroid in traveling electric field. *Biomicrofluidics*, 4, 1, (March 2010), ISSN 1932-1058.

Cheng, I.F., Chung, C.C., & Chang, H.C. (2011). High-throughput electrokinetic bioparticle focusing based on a travelling-wave dielectrophoretic field. *Microfluidics and Nanofluidics*, 10, 3, (March 2011), pp. 649-660, ISSN 1613-4982.

Cleveland Clinic Foundation. (n.d.).What is Chemotherapy, In: Chemocare.com, September 2010, Available from: <http://www.chemocare.com/whatis/how_do_the_doctors_decide_which.asp>.

Donnelly, R.F., Majithiya, R., Singh, T.R.R., Morrow, D.I.J., Garlad, M.J., Demir, Y.K., Migalska, K., Ryan, E., Gillen, D., Scott, C.J., & Woolfson, A.D. (2011). Design, optimization and characterisation of polymeric microneedle arrays prepared by a novel laser-based micromoulding technique. *Pharmaceutical Research*, 28, 1, (January 2011), pp. 41-57, ISSN 0724-8741.

Durr, M., Kentsch, J., Muller, T., Schnelle, T., & Stelzle, M. (2003). Microdevices for manipulation and accumulation of micro- and nanoparticles by dielectrophoresis. *Electrophoresis*, 24, 4, (February 2003), pp. 722-731, ISSN 0173-0835.

Elman, N.M., Duc, H.L.H., & Cima, M.J. (2009). An implantable MEMS drug delivery device for rapid delivery in ambulatory emergency care. *Biomedical Microdevices*, 11, 3, (June 2009), pp. 625-631, ISSN 1387-2176.

Escobar-Chavez, J.J., Bonilla-Martinez, D., Villegas-Gonzalez, M.A., Molina-Trinidad, E., Casas-Alancaster, N., & Revilla-Vazquez, A.L. (2011). Microneedles: a valuable physical enhancer to increase transdermal drug delivery. *Journal of Clinical Pharmacology*, 51, 7, (July 2011), pp. 964-977, ISSN 0091-2700.

Farokhzad, O.C., Dimitrakov, J.D., Karp, J.M., Khademhosseini, A., Freeman, M.R., & Langer, R. (2006). Drug delivery systems in urology – getting "smarter". *Urology*, 68, 3, (September 2006), pp. 463-469,ISSN 0090-4295.

Felten, M., Staroske, W., Jaeger, M.S., Schwille, P., & Duschl, C. (2008). Accumulation and filtering of nanoparticles in microchannels using electrohydrodynamically induced vertical flows. *Electrophoresis*, 29, 14, (July 2008), pp. 2987-2996, ISSN 0173-0835.

Ha, J.W., & Yang, S.M. (1999). Breakup of a multiple emulsion drop in a uniform electric field. *Journal of Colloid and Interface Science,* 213, (May 1999), pp. 92–100, ISSN: 0021-9797.

Hamouda, T., Hayes, N.M., Cao, Z.Y., Tonda, R., Johnson, K., Wright, D.C., Brisker, J., & Baker, J.R. (1999). A novel surfactant nanoemulsion with broad-spectrum sporicidal activity against bacillus species. *Journal of Infectious Diseases,* 180, 6, (December 1999), pp. 1939-1949, ISSN 0944-5013.

Hershock, D. (2006). Medical and Surgical Therapy for Gastric Cancer, In: Endoscopic Oncology, Faigel, D.O. and Kochman, M.L., pp. 173-181, Humana Press, Retrieved from <http://www.crcnetbase.com/search/advanced>.

Jensen, K. & Lee, A. (2004). The science & applications of droplets in microfluidic devices – Foreword. *Lab On A Chip*, 4, 4, (n.d.), pp. 31N-32N, ISSN 1473-0189.

Kang, Y. & Li, D. (2009). Electrokinetic motion of particles and cells in microchannels. *Microfluidics and Nanofluidics*, 6, 4, (April 2009), pp. 431-460, ISSN 1613-4982.

Kim, H., Luo, D.W., Link, D., Weitz, D.A., Marquez, M., & Cheng, Z.D. (2007). Controlled production of emulsion drops using an electric field in a flow-focusing microfluidic device. *Applied Physics Letters*, 91, 13, (September, 2007), pp.133106, ISSN 0003-6951.

Kim, S.H., Kim, J.W., Cho, J.C., & Weitz, D.A. (2011). Double-emulsion drops with ultra-thin shells for capsule templates. *Lab Chip*, 2011, 11, 18, (2011), pp. 3162-3166, ISSN 1473-0197.

Kiss, N., Brenn, G., Pucher, H., Wieser, J., Scheler, S., Jennewein, H., Suzzi, D., & Khinast, J. (2011). Formation of O/W emulsions by static mixers for pharmaceutical applications. *Chemical Engineering Science,* 66, 21, (November 2011), pp. 5084-5094, ISSN: 0009-2509.

Kirby, B.J., & Hasselbrink, E.F. (2004). Zeta potential of microfluidic substrates: 2. Data for polymers. *Electrophoresis*, 25, 2, (January 2004) pp. 203–213, ISSN: 0173-0835.

Lee, K., Lee, C.Y., & Jung, H. (2011). Dissolving microneedles for transdermal drug administration prepared by stepwise controlled drawing of maltose. *Biomaterials*, 32, 11, (April 2011), pp. 3134-3140, ISSN 0142-9612.

Lee, W., Walker, L.M., & Anna, S.L. (2009). Role of geometry and fluid properties in droplet and thread formation processes in planar flow focusing. Physics of Fluids, 21, 3, (March 2009), ISSN 1070-6631.

Levi, J.A., Dalley, D.N., & Aroney, R.S. (1979). Improved combination chemotherapy in advanced gastric-cancer. *British Medical Journal*, 2, 6203, (December 1979), pp. 1471-1473, ISSN 0959-8138.

Liao, C.Y., & Su, Y.C. (2010). Formation of biodegradable microcapsules utilizing 3D, selectively surface-modified PDMS microfluidic devices. *Biomedical Microdevices*, 12, 1, (February 2010), pp. 125-133, ISSN: 1387-2176.

Lima, J.L.F.C., Santos, J.L.M., Dias, A.C.B., Ribeiro, M.F.T, & Zagatto, E.A.G. (2004). Multi-pumping flow systems: an automation tool. *Talanta,* 64, 5, (December 2004), pp. 1091–1098, ISSN: 0039-9140.

Lin, J.T.Y., & Yeow, J.T.W. (2007). Enhancing dielectrophoresis effect through novel electrode geometry. *Biomedical Microdevices*, 9, 6, (December 2007), pp. 823-831, ISSN 1387-2176.

Lv, Y.G., Liu, J., Gao, Y.H., & Xu, B. (2006). Modeling of transdermal drug delivery with a microneedle array. Journal of Micromechanics and Microengineering, 16, 11, (November 2006), pp. 2492-2501, ISSN 0960-1317.

Martin-Banderas, L., Flores-Mosquera, M., Riesco-Chueca, P., Rodriguez-Gil, A., Cebolla, A., Chavez, S., & Ganan-Calvo, A.M. (2005). Flow Focusing: A Versatile Technology to Produce Size- Controlled and Specific-Morphology Microparticles. *Small*, 1, 7, (July 2005), pp. 688-692. ISSN: 1613-6810.

Mejia, A.F., He, P., Luo, D.W., Marquez, M., & Cheng, Z.D. (2009). Uniform discotic wax particles via electrospray emulsification, *Journal of Colloid and Interface Science*, 334, 1, (June 2009), pp. 22-28, ISSN: 0021-9797.

Mezzenga, R., Schurtenberger, P., Burbidge, A., & Michel, M. (2005), Understanding foods as soft materials. *Nature Materials*, 4, 10, (October 2005), pp. 729-740, ISSN: 1476-1122.

Migalska, K., Morrow, D.I.J., Garland, M.J., Thakur, R., Woolfson, A.D., &, Donnelly, R.F. (2011). Laser-engineered dissolving microneedle arrays for transdermal macromolecular drug delivery. *Pharmaceutical Research*, 28, 8, (August 2011), pp. 1919-1930, ISSN 0724-8741.

Minerick, A.R. (2008). The rapidly growing field of micro and nanotechnology to measure living cells. *AIChE Journal*, 54, 9, (September 2008), pp. 2230-2237, ISSN 0001-1541.

Moon, S., & Lee, S.S. (2003). Fabrication of microneedle array using inclined LIGA process. Transducer'03 12th International Conference on Solid-State Sensors, Actuators and Microsystems, 2, (n.d.), pp. 1546-1549.

National Cancer Institute. (n.d.). Stomach Cancer, In: *National Institute of Health*, September 2010, Available from: <http://www.cancer.gov/cancertopics/types/stomach>.

Nguyen, N.T., & Wereley, S.T. (2006). *Fundamentals and Applications of Microfluidics* (2nd Edition), Artech House, ISBN 1580539726, Boston.

Pacek, A.W., Chamsart, S., Nienow, A.W., & Bakker, A. (1999). The influence of impeller type on mean drop size and drop size distribution in an agitated vessel. *Chemical Engineering Science* 54, 19 (October 1999), pp. 4211-4222, ISSN: 0009-2509.

Pai, S.A., Rivankar, S.H., & Kocharekar, S.S. (2003). Parenteral cisplatin emulsion. United States Patent, US 6,572,884, date of filling (June 14, 2002), date of issue(June 3, 2003).

Pethig, R. (2010). Dielectrophoresis: status of the theory, technology, and applications. *Biomicrofluidics*, 4, 3, (September 2010), ISSN 1932-1058.

Power, D.G., Kelsen, D.P., & Shah, M.A. (2010). Advanced gastric cancer – slow but steady progress. Cancer Treatment Reviews, 36, 5, (August 2010), pp. 384-392, ISSN 0305-7372.

Rivera, F., Vega-Villegas, M.E., & Lopez-Brea, M.F. (2007). Chemotherapy of advanced gastric cancer. *Cancer Treatment Reviews*, 33, 4, (June 2007), pp. 315-324, ISSN 0305-7372.

Santini, J.T., Cima, M.J., & Langer, R.S. (1999). A controlled-release microchip. *Nature*, 397, 6717, (January 1999), pp. 335-338, ISSN0028-0836.

Santini, J.T., Richards, A.C., Scheidt, R.A., Cima, M.J., & Langer, R.S. (2000). Microchip technology in drug delivery. *Annals of Medicine*, 32, 6, (September 2000), pp. 377-379, ISSN 0785-3890.

Seo, M., Paquet, C., Nie, Z., Xu, S.Q., & Kumacheva, C. (2007). Microfluidic consecutive flow-focusing droplet generators. *Soft Matter*, 3, 8, (May 2007), pp. 986–992, ISSN: 1744-683X.

Soller, E., Murray, C., Maoddi, P., & Di Carlo, D. (2011). Rapid prototyping polymers for microfluidic devices and high pressure injections. *Lab on a chip, 22,* (November 2011), pp. *3752-65,* ISSN: 1473-0189.

Srivastava, S.K., Gencoglu, A., & Minerick, A.R. (2011). DC insulator dielectrophoretic applications in microdevice technology: a review. *Analytical and Bioanalytical Chemistry*, 399, 1, (January 2011), pp. 301-321, ISSN 1618-2642.

Thiele, J., Steinhauser, D., Pfohl, T., & Foster, S. (2010). Preparation of monodisperse block copolymer vesicles via flow focusing in microfluidics. *Langmuir*, 26, 9, (May 2010), pp. 6860-6863, ISSN 0743-7463.

Utada. A.S., Lorenceau, E., & Link, D.R. (2005), Monodisperse double emulsions generated from a microcapillary device. *Science*, 308, 5721, (April 2005), pp. 537-541, ISSN: 0036-8075

Vergauwe, N., Witters, D., Ceyssens, F., Vermeir, S., Verbruggen, B., Puerr, R., & Lammertyn, J. (2011). A versatile electrowetting-based digital microfluidic platform for quantitative homogeneous and heterogeneous bio-assays. *Journal of Micromechanics and Microengineering*, 21, 5, (May 2011), ISSN 0960-1317.

Wang, C., Wang, X., & Jiang, Z. (2011). Dielectrophoretic driving of blood cells in a microchannel. *Biotechnology and Biotechnological Equipment*, 25, 2, (May 2011), pp. 2405-2411, ISSN 1310-2818.

Wang, P.M., Cornwell, M., Hill, J., & Prausnitz, M.R. (2006). Precise microinjection into skin using hollow microneedles. *Journal of Investigative Dermatology*, 126, 5, (May 2006), pp. 1080-1087, ISSN 0022-202X.

Weng, C.H., Huang, T., Huang, C., Yeh, C., Lei, H., & Lee, G. (2011). A suction-type microfluidic immunosensing chip for rapid detection of the dengue virus. *Biomedical Microdevices*, 13, 3, (June 2011), pp. 585-595, ISSN 1387-2176.

Wibowo, C., & Ng, K.M. (2001). Product-Oriented Process Synthesis and Development: Creams and Pastes. *AIChE Journal*, 47, 12, (December 2001), ISSN: 0001-1541.

Xiao, Z.G., & Young, E.F.Y. (2011). Placement and routing for cross-referencing digital microfluidic biochips. *IEEE Transactions on Computer-Aided Design of Integrated Circuits and Systems*, 30, 7, (July 2011), pp. 1000-1010, ISSN 0278-0070.

Zagnoni, M., Baroud, C.N., & Cooper, J.M. (2009). Electrically initiated upstream coalescence cascade of droplets in a microfluidic flow. *Physical Review E*, 80, 4, (October 2009), pp. 046303, ISSN: 1539-3755.

Zagnoni, M., Lain, G.L., & Cooper, J.M. (2010). Electrocoalesence mechanisms of microdroplets using localized electric fields in microfluidic channels. *Langmuir*, 26, 18, (September 2010), pp. 14443-14449, ISSN 0743-7463.

Zahn, J.D., Deshmukh, A., Pisano, A.P., & Liepmann, D. (2004). Continuous on-chip micropumping for microneedle enhanced drug delivery. *Biomedical Microdevices*, 6, 3, (September 2004), pp. 183-190, ISSN 1387-2176.

Zhu, H., Mayandad, S., Coskun, A.F., Yagidere, O., & Ozcan, A. (2011). Optofluidic fluorescent imaging cytometry on a cell phone. *Analytical Chemistry*, 83, 17, (September 2011), pp. 6641-6647, ISSN 0003-2700.

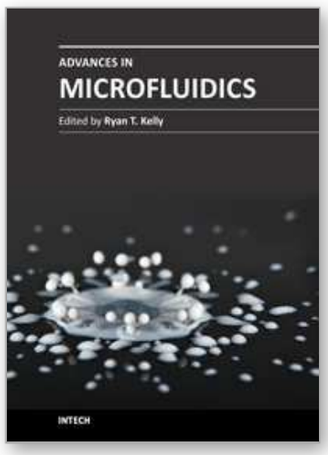


**Advances in Microfluidics**

Edited by Dr. Ryan Kelly

ISBN 978-953-51-0106-2
Hard cover, 250 pages
**Publisher** InTech
**Published online** 07, March, 2012
**Published in print edition** March, 2012

Advances in Microfluidics provides a current snapshot of the field of microfluidics as it relates to a variety of sub-disciplines. The chapters have been divided into three sections: Fluid Dynamics, Technology, and Applications, although a number of the chapters contain aspects that make them applicable to more than one section. It is hoped that this book will serve as a useful resource for recent entrants to the field as well as for established practitioners.

**How to reference**

In order to correctly reference this scholarly work, feel free to copy and paste the following:

Tayloria Adams, Chungja Yang, John Gress,Nick Wimmer and Adrienne R. Minerick (2012). A Tunable Microfluidic Device for Drug Delivery, Advances in Microfluidics, Dr. Ryan Kelly (Ed.), ISBN: 978-953-51-0106-2, InTech, Available from: http://www.intechopen.com/books/advances-in-microfluidics/exploring-a-digital-microfluidic-device-for-gastric-cancer-drug-delivery

INTECH
open science | open minds

**InTech Europe**
University Campus STeP Ri
Slavka Krautzeka 83/A
51000 Rijeka, Croatia
Phone: +385 (51) 770 447
Fax: +385 (51) 686 166
www.intechopen.com

**InTech China**
Unit 405, Office Block, Hotel Equatorial Shanghai
No.65, Yan An Road (West), Shanghai, 200040, China
中国上海市延安西路65号上海国际贵都大饭店办公楼405单元
Phone: +86-21-62489820
Fax: +86-21-62489821

IntechOpen